

Developmental Cell, Volume 46

Supplemental Information

Nrf2-Mediated Fibroblast Reprogramming Drives

Cellular Senescence by Targeting the Matrisome

Paul Hiebert, Mateusz S. Wietecha, Michael Cangkrama, Eric Haertel, Eleni Mavrogonatou, Michael Stumpe, Heiko Steenbock, Serena Grossi, Hans-Dietmar Beer, Peter Angel, Jürgen Brinckmann, Dimitris Kletsas, Jörn Dengjel, and Sabine Werner

Figure S1. Related to Figures 1 and 2.

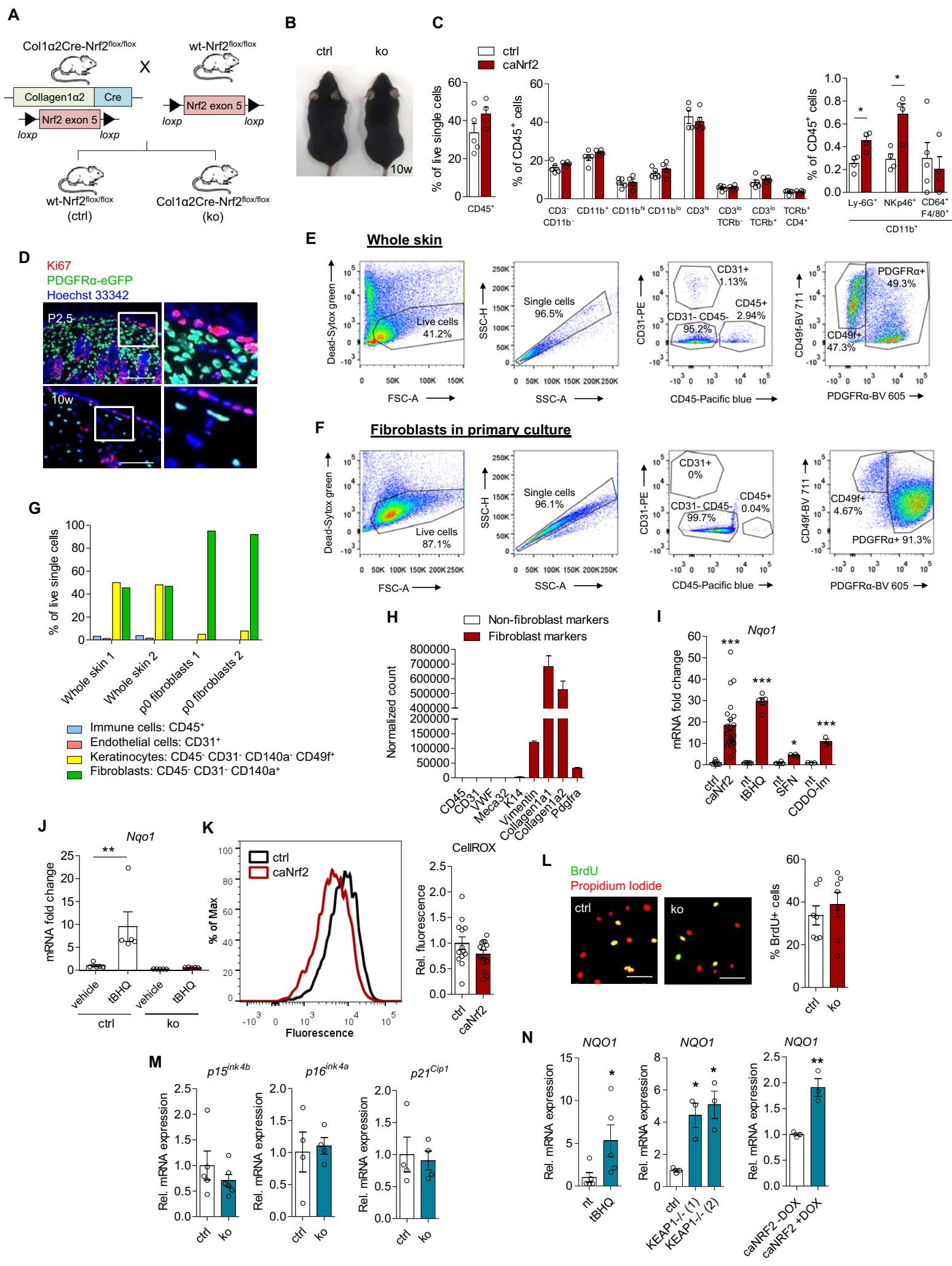


Figure S1. Characterization of mice with Nrf2 gain- and loss-of-function in fibroblasts. Related to Figures 1 and 2.

(A) Scheme depicting the generation of mice lacking Nrf2 in fibroblasts. (B) Macroscopic appearance of ko vs ctrl mice at 10 weeks of age. (C) Flow-cytometric analysis of the immune cell composition in back skin from mice during homeostasis at 10 weeks of age. (D) Skin sections from PDGFR α -eGFP transgenic mice at P2.5 and 10 weeks of age stained for Ki67, demonstrating a lack of proliferating fibroblasts in the skin during homeostasis. (E) – (G) Flow-cytometric analysis of (E) whole skin from mice at P2.5 and (F) freshly isolated and cultured primary fibroblasts from P2.5 mouse back skin. (G) The percentage of different cell types in whole skin or freshly isolated fibroblast cultures. (H) Gene expression of fibroblast and non-fibroblast markers at passage 2 based on RNA-seq data. (I) Relative expression of *Nqo1* by caNrf2 (N=7-22 cultures per genotype from different mice) and wild-type fibroblasts treated with tBHQ (N=5), SFN (N=4) or CDDO-Im (N=3). (J) Relative expression of *Nqo1* in fibroblasts at passage 2 isolated from ko vs ctrl mice treated with either vehicle or tBHQ (N=5 cultures per genotype from different mice). (K) ROS detection in caNrf2 vs ctrl fibroblasts using the CellROX® Orange ROS detection kit (N=13). (L) BrdU incorporation and immunostaining on fibroblasts from ko vs ctrl mice at passage 2 (N=7). (M) Gene expression of senescence markers *p15ink4b*, *p16ink4a* and *p21Cip1* in ko vs ctrl fibroblasts at passage 2. Bar graphs shown mean and SEM. *** $P < 0.001$, ** $P < 0.01$, * $P < 0.05$, Mann-Whitney U test (C, I, M, N) or 2-way ANOVA with Bonferroni posttest (J). Scale bars = 100 μ m (D) and 50 μ m (L).

Figure S2. Related to Figure 4.

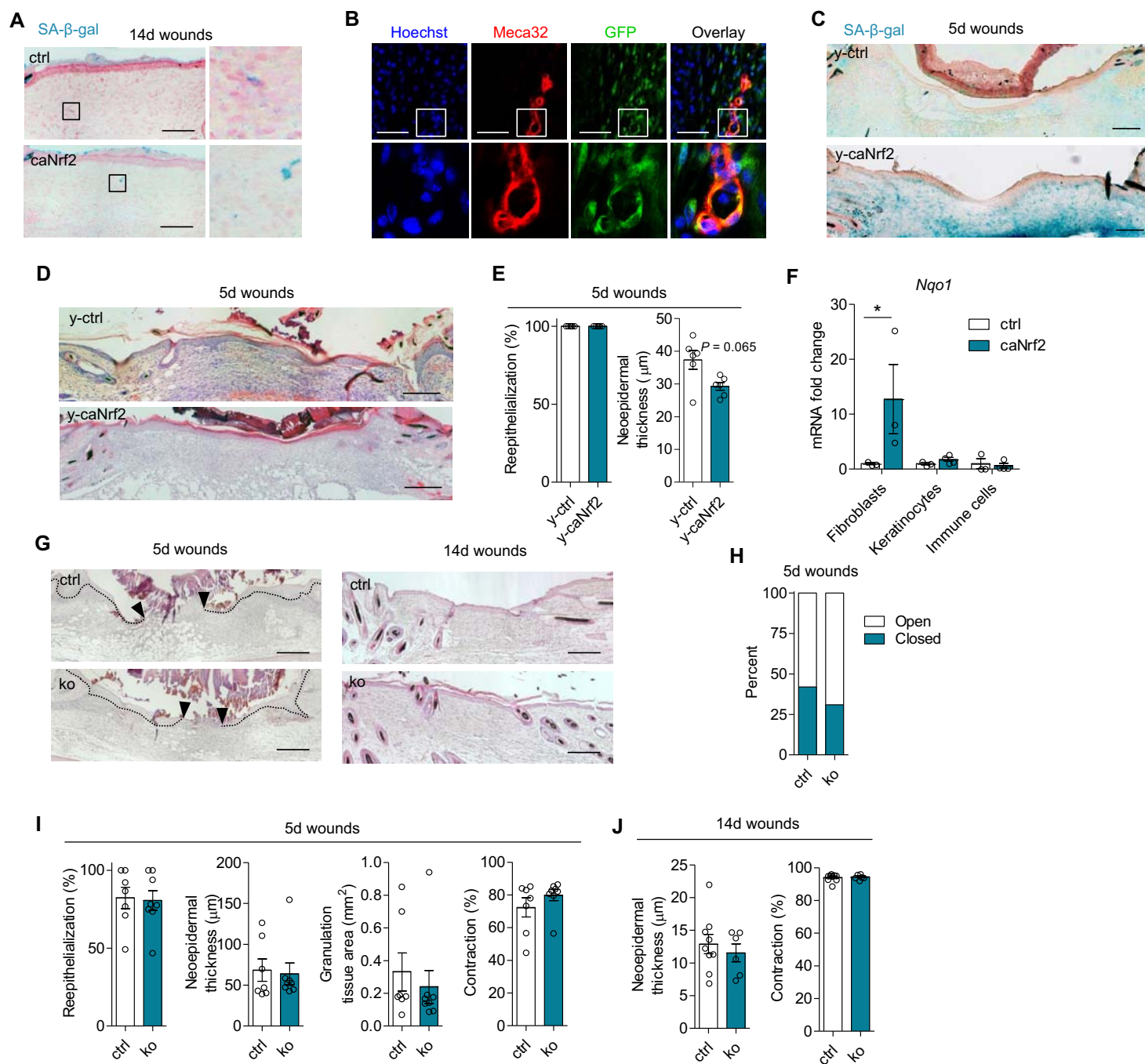


Figure S2. Normal wound healing in mice with Nrf2 deficiency in fibroblasts and wound healing in young caNrf2-transgenic mice. Related to Figure 4.

(A) Examination of wounds from 10 week-old ctrl and caNrf2 mice at 14 days post wounding using SA- β -gal histochemistry. (B) Co-immunofluorescence staining of blood vessels in the granulation tissue for the endothelial marker Meca32 and GFP (reflecting transgene expression). Nuclei were counterstained with Hoechst. (C,D) Examination of wounds from 4 week-old (young) ctrl (y-ctrl) and caNrf2 (y-caNrf2) mice at 5 days post wounding using SA- β -gal histochemistry (C) or hematoxylin & eosin staining (D). (E) Quantification of reepithelialization and neoepidermal thickness in 5-day wounds of ctrl and caNrf2 mice at the age of 4 weeks (N=3 mice, n=6 wounds). (F) Expression of *Nqo1* in FACS-isolated cells from 5-day wounds of caNrf2 vs ctrl mice (N=3-4 mice; n=3-4 wounds). * $P < 0.05$, 2-way ANOVA with Bonferroni posttest. (G) Representative histological sections of 5-day and 14-day wounds from ko and ctrl mice stained with hematoxylin and eosin. Arrow heads point to the edge of the migrating epithelium. (H) Quantification of the number of open/closed wounds from ko vs ctrl mice (N=5-7; n=5-7). (I) Morphometric analysis of 5-day (N=7-8; n=7-8) and (J) 14-day (N=6-9; n=6-9) wounds from ko vs ctrl mice. Bar graphs show mean and SEM. Scale bars = 100 μ m.

Figure S3. Related to Figure 4.

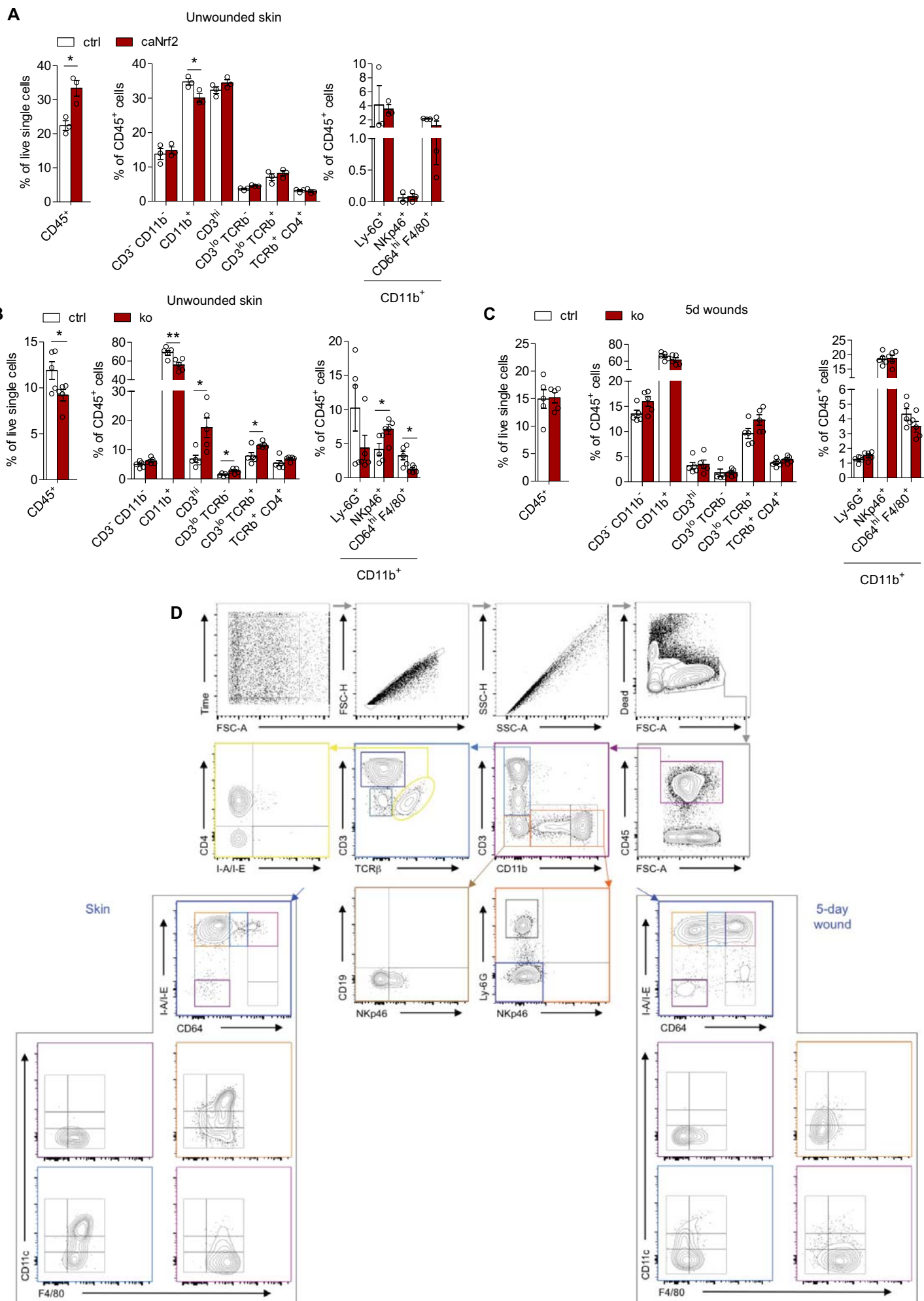


Figure S3. Immune cell composition in unwounded skin and 5d wounds. Related to Fig. 4. (A) Flow-cytometric analysis of the immune cell composition in unwounded skin from caNrf2 and ctrl mice, (B) 5 day wounds from ko and ctrl mice and (C) unwounded skin from ko and ctrl mice. Bar graphs show mean and SEM. (D) Gating strategy used for profiling of immune cells in wounds and unwounded skin.

Figure S4. Related to Figures 5 and 6.

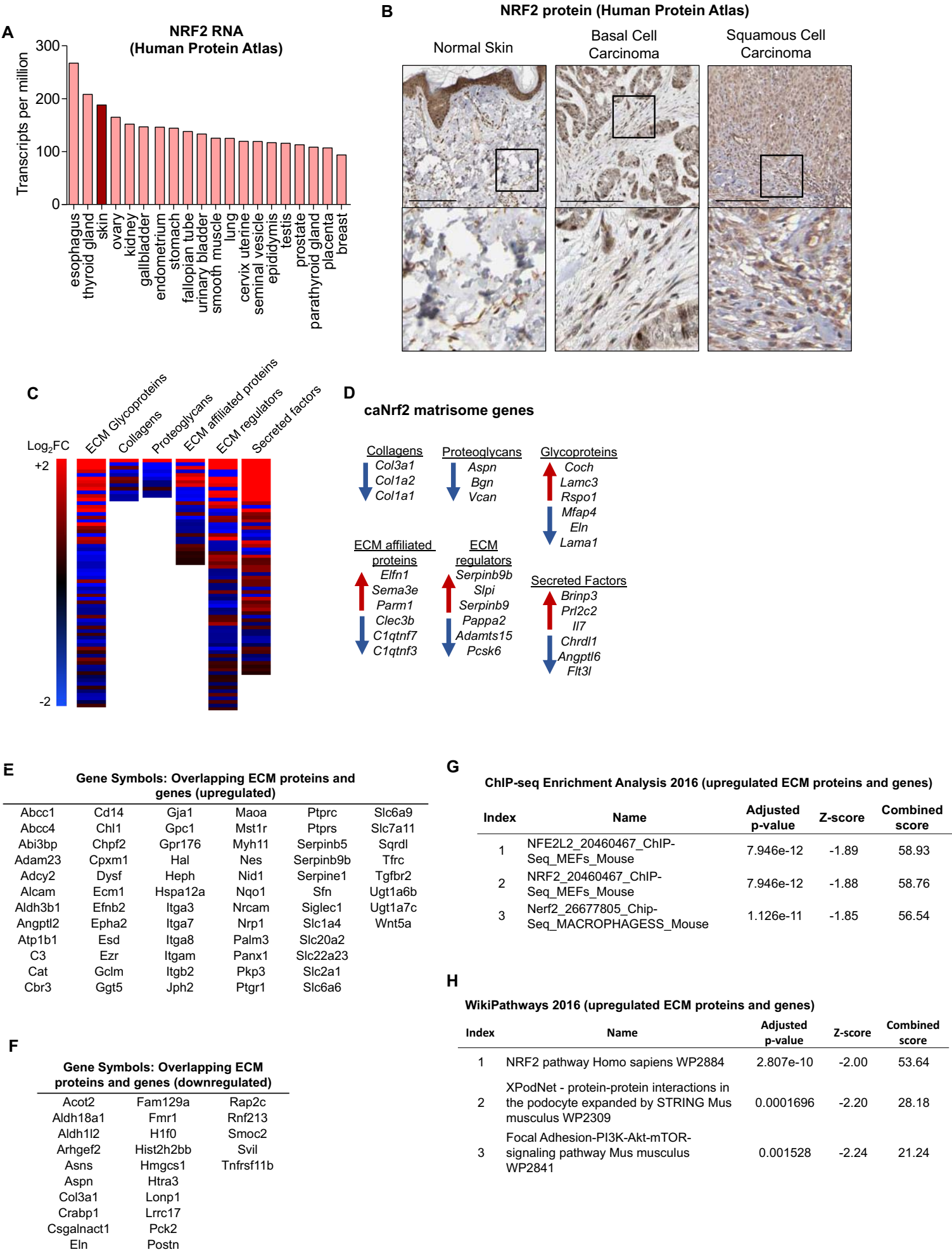


Figure S4. Altered expression and deposition of ECM genes in caNrf2 fibroblasts. Related to Figures 5 and 6.

(A) Data from the Human Protein Atlas showing *NRF2* (*NFE2L2*) gene expression in transcripts per million from different tissues. (B) Immunohistochemistry images from the Human Protein Atlas showing NRF2 expression in normal skin (<https://www.proteinatlas.org/ENSG00000116044-NFE2L2/tissue>), basal cell carcinoma and cutaneous squamous cell carcinoma (<https://www.proteinatlas.org/ENSG00000116044-NFE2L2/pathology/tissue/skin+cancer#ihc>). Scale bars = 200 μ m. (C) Heat maps of differentially expressed genes identified by RNA-seq in caNrf2 fibroblasts corresponding to matrisome categories. (D) List of differentially expressed genes identified by RNA-seq in caNrf2 fibroblasts corresponding to matrisome categories. (E, F) List of genes upregulated (E) or downregulated (F) in caNrf2 fibroblasts that are also upregulated or downregulated ECM components according to the mass spectrometry data. (G) ChIP-seq enrichment analysis comparing upregulated ECM proteins deposited by caNrf2 fibroblasts to previously published ChIP-seq datasets. (H) Comparison of ECM proteins deposited to a larger extent by caNrf2 compared to ctrl fibroblasts with known cellular pathways using Wikipathways.

Figure S5. Related to Figure 6.

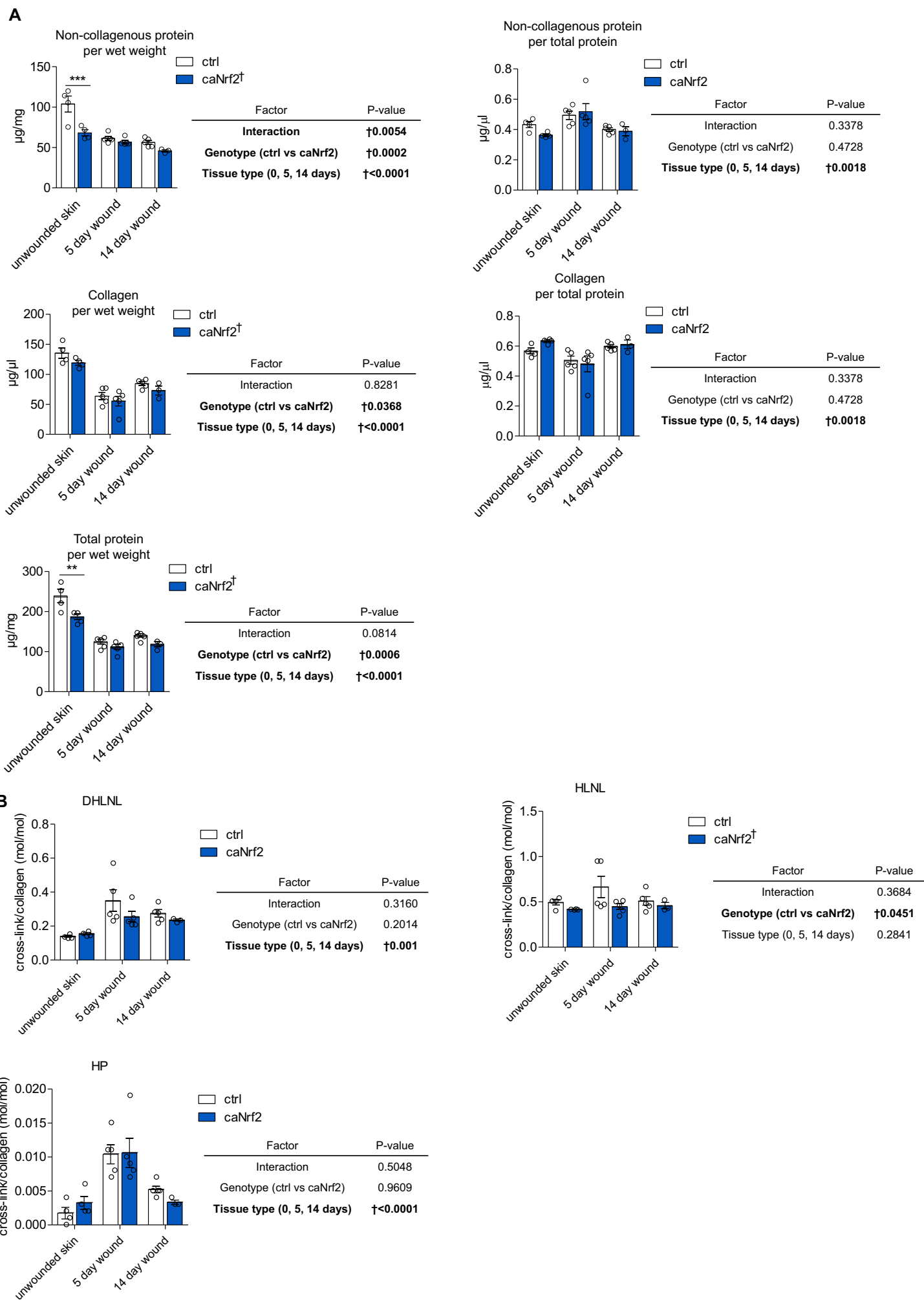


Figure S5. Biochemical analysis of collagen content and cross-linking. Related to Figure 6. (A) Collagen analysis and (B) analysis of collagen cross-linking in unwounded skin and in 5 and 14 day wounds from caNrf2 vs ctrl mice (N=4-5 mice; n=4-5 wounds, caNrf2 14d N=3; n=3). Bar graphs show mean and SEM. ** $P < 0.01$, * $P < 0.05$; 2-way ANOVA with Bonferroni posttest.

Figure S6. Related to Figure 7.

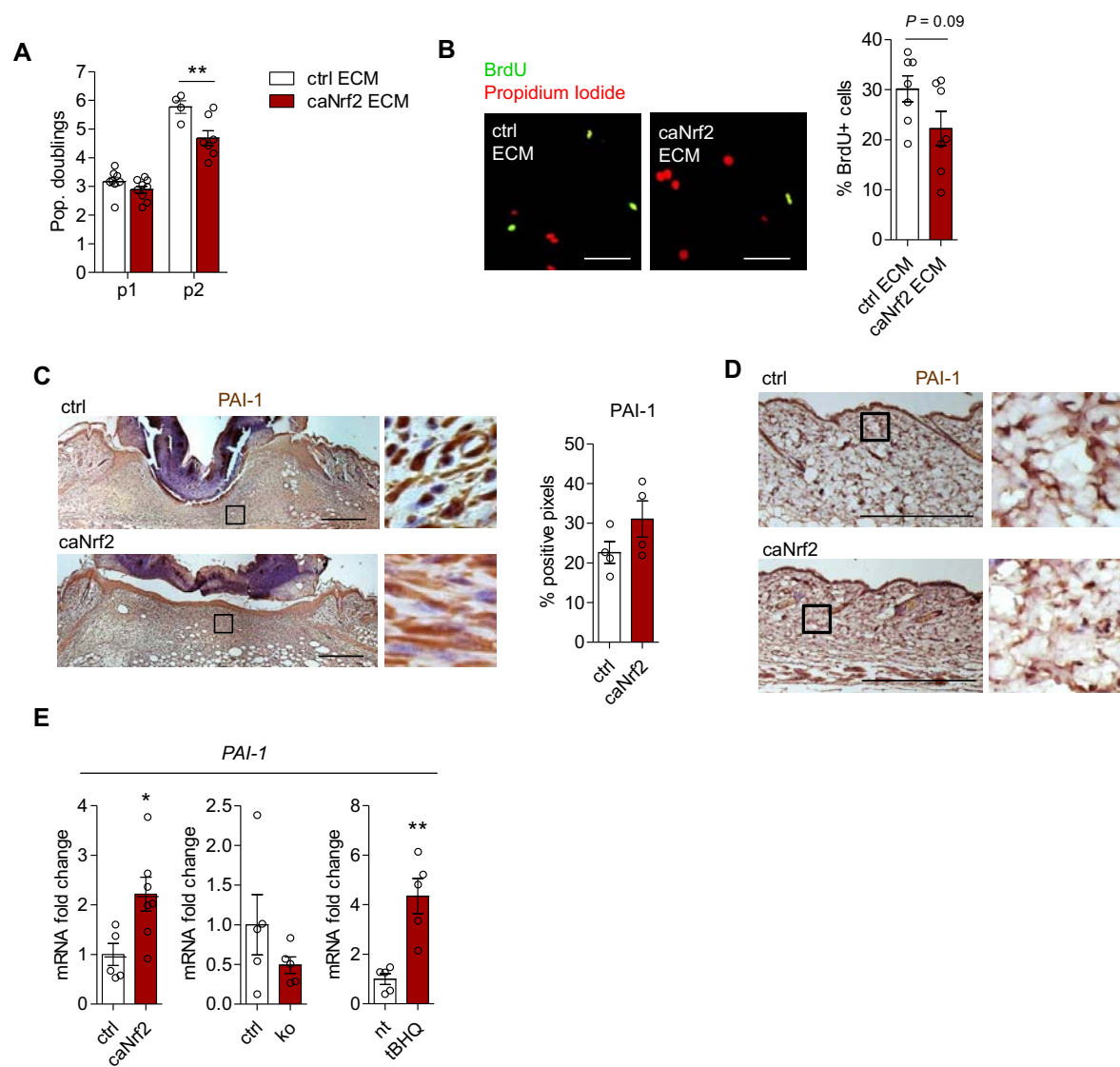


Figure S6. Nrf2 targets the extracellular matrix to promote fibroblast senescence. Related to Figure 7.

Skin fibroblasts were isolated from wild-type mice and directly plated onto dishes coated with ECM deposited by either ctrl or caNrf2 fibroblasts. Cells were plated onto new ECM-coated dishes during each passage. (A) Population doublings over 2 passages calculated by counting trypan blue excluding cells (N=4-7 ECM-coated dishes from fibroblasts isolated from different mice). (B) BrdU incorporation and staining of fibroblasts at passage 2 (N=7). (C) PAI-1 immunohistochemistry performed on 5-day wounds and quantification of positive pixels (N=4 mice). (D) PAI-1 immunohistochemistry performed on sections from unwounded skin of mice at 10 weeks of age. (E) qRT-PCR analysis of *PAI-1* gene expression in ctrl, caNrf2, ko and wild-type fibroblasts treated with tBHQ (N=5-7 cultures per genotype from different mice). Bar graphs show mean and SEM. *P<0.05, **P<0.01; 2-way ANOVA with Bonferroni posttest (A) or Mann-Whitney U test (E). Scale bars = 50 μ m (B) or 200 μ m (C,D).

Figure S7. Related to Star Methods.

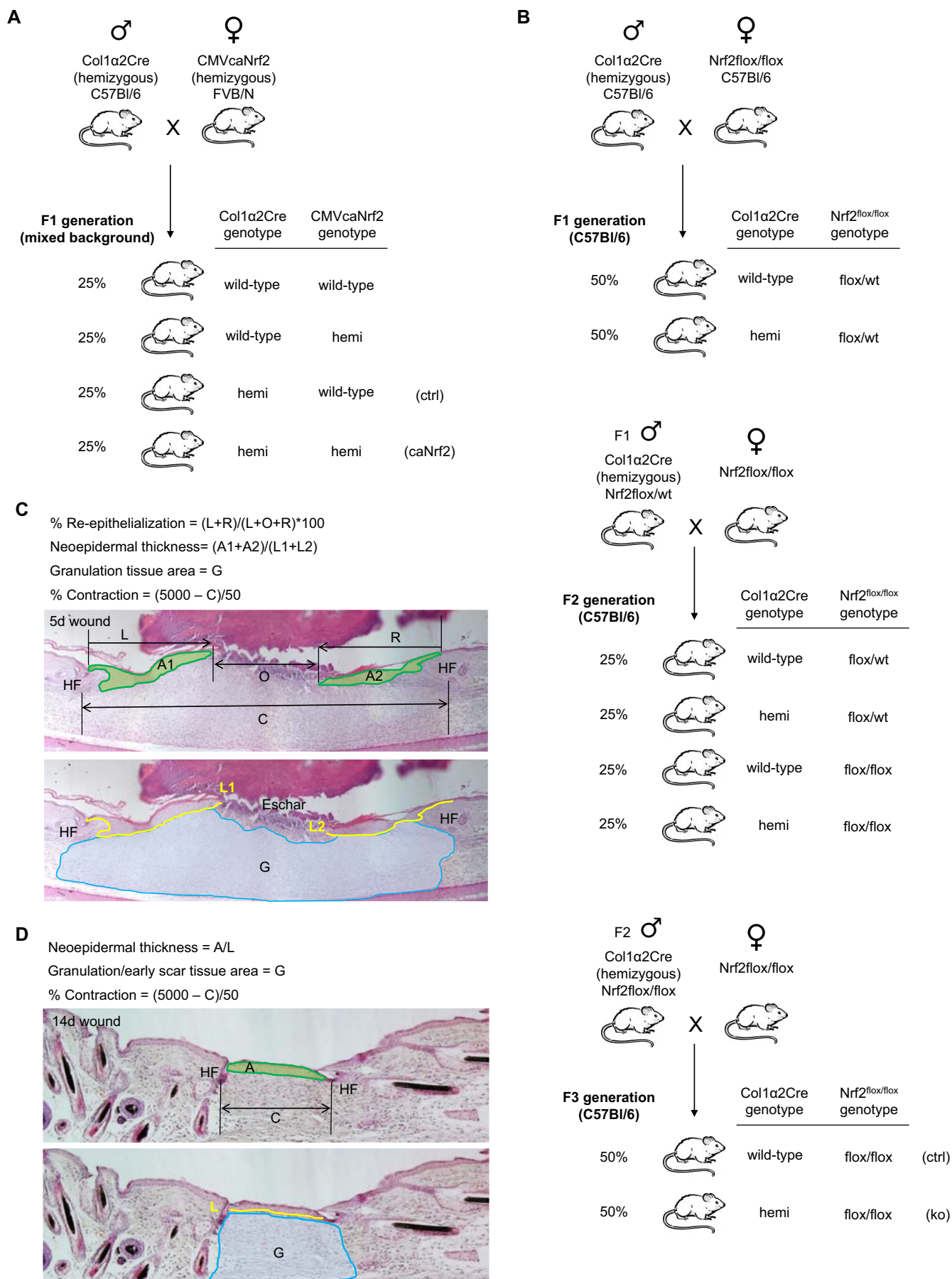


Figure S7. Related to Star Methods.

Generation of mice with Nrf2 gain- or loss-of-function in fibroblasts and schematic representation of the parameters determined in the histomorphometric analysis of wounds.

(A) Scheme depicting the breeding and control animals used in experiments with caNrf2 mice/fibroblasts (hemi = hemizygous). (B) Scheme depicting the breeding and control animals used in experiments with ko mice/fibroblasts (hemi = hemizygous). (C,D) Scheme depicting a 5 day (C) and a 14 day (D) wound and the parameters determined in the histomorphometric analysis of the wounds.

Table S3. Gene Ontology Enrichment Analysis (Cellular Component). Related to Figure 6.**Both up/down-regulated genes**

Term ID	Description	log10 p-value
GO:0005576	extracellular region	-36.0011
GO:0005615	extracellular space	-28.1561
GO:0070062	extracellular exosome	-11.9206
GO:0005578	proteinaceous extracellular matrix	-12.9712
GO:0031012	extracellular matrix	-8.5018
GO:0009986	cell surface	-8.3339
GO:0016020	membrane	-10.4194
GO:0043235	receptor complex	-5.254
GO:0005887	integral component of plasma membrane	-6.7262
GO:0005829	cytosol	-6.4776
GO:0016021	integral component of membrane	-17.5721
GO:0001527	microfibril	-6.0769
GO:0005604	basement membrane	-5.2479
GO:0005886	plasma membrane	-21.5844
GO:0009897	external side of plasma membrane	-5.6706

Up-regulated genes

Term ID	Description	log10 p-value
GO:0005576	extracellular region	-14.5787
GO:0005829	cytosol	-11.094
GO:0016020	membrane	-11.4857
GO:0045121	membrane raft	-4.492
GO:0070062	extracellular exosome	-20.6063
GO:0005615	extracellular space	-18.9521
GO:0009986	cell surface	-9.0261
GO:0005887	integral component of plasma membrane	-4.8389
GO:0016021	integral component of membrane	-11.8602
GO:0005737	cytoplasm	-4.9109
GO:0043292	contractile fiber	-4.0612
GO:0005886	plasma membrane	-21.4293
GO:0009897	external side of plasma membrane	-4.4881

Down-regulated genes

Term ID	Description	log10 p-value
GO:0005576	extracellular region	-17.1548
GO:0005578	proteinaceous extracellular matrix	-9.2326
GO:0005615	extracellular space	-6.4988
GO:0001527	microfibril	-6.1055
GO:0031012	extracellular matrix	-6.2915
GO:0016021	integral component of membrane	-4.8247

Table S3. Gene Ontology Enrichment Analysis (Cellular Component). Related to Figure 6.

List of the most significant results obtained from gene ontology enrichment analysis performed by EdgeR software. Enriched gene ontology terms listed are those with \log_{10} p-value < -4 .